# Search for the QCD Critical Point with Beam Energy Scan at RHIC

## Status and Prospect

Xiaofeng Luo

May 7-8, 2019

Central China Normal University

# QCD Phase Diagram

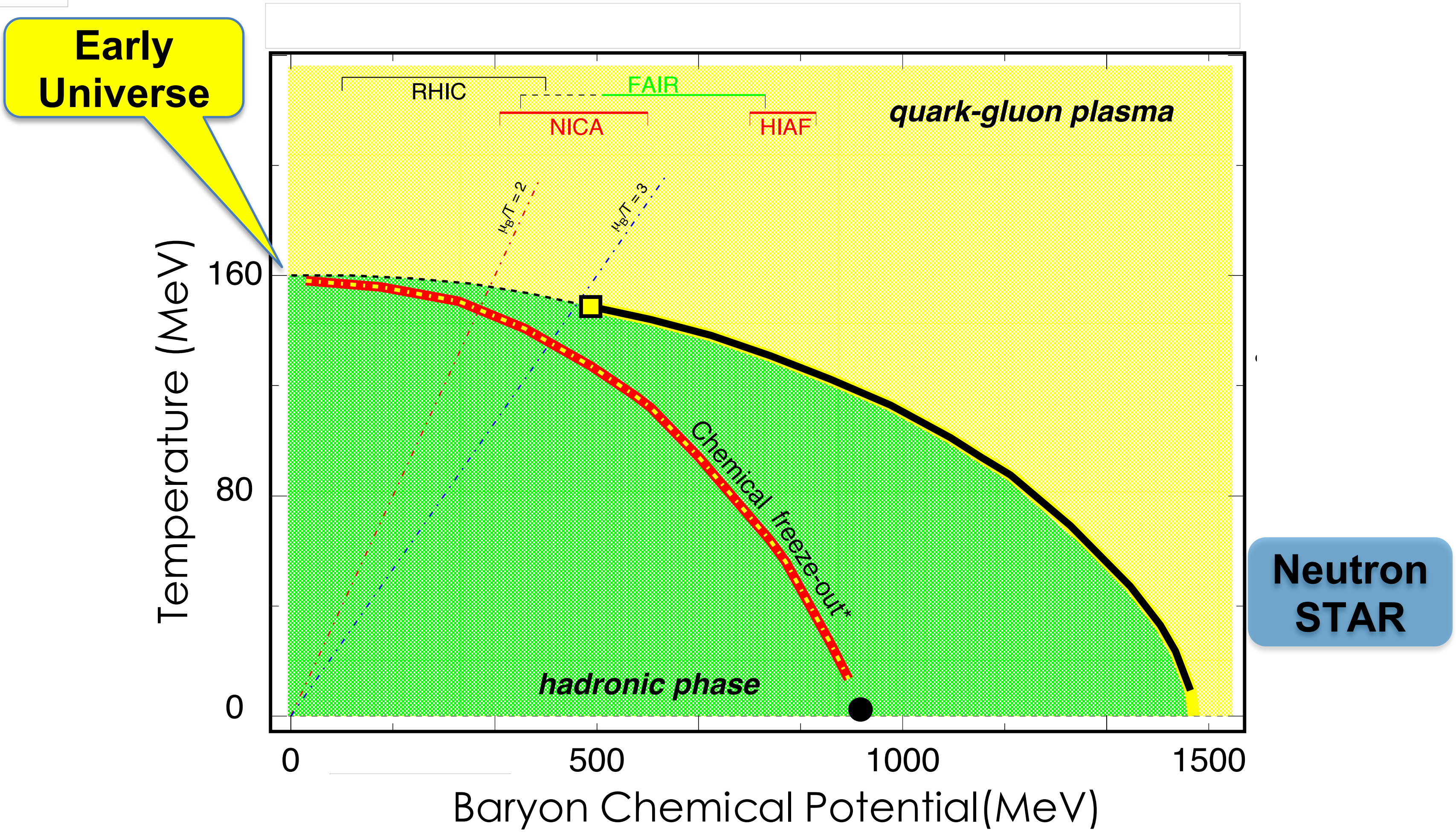


**One of the Key Problems: Can we find the QCD critical point and its location ?**

# Location of CEP: Theoretical Prediction

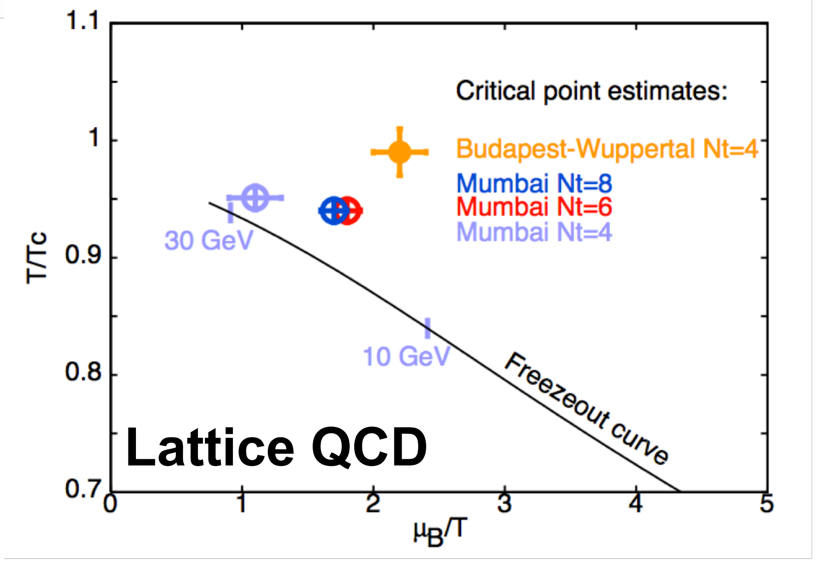


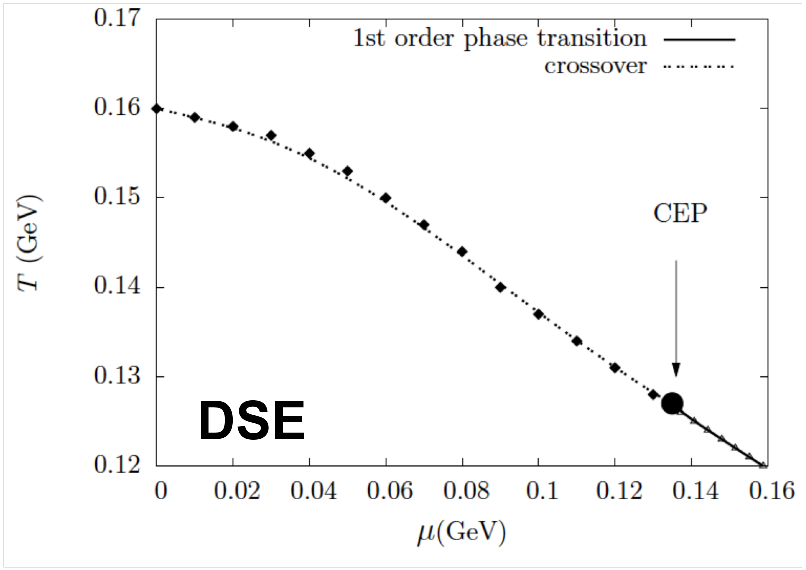


**Lattice QCD:**

1): Fodor&Katz, JHEP 0404,050 (2004):
$(\mu^E_B, T_E) = (360, 162)$ MeV (Reweighting)

2): Gavai&Gupta, NPA 904, 883c (2013)
$(\mu^E_B, T_E) = (279, 155)$ MeV (Taylor Expansion)

3): F. Karsch et al. NPA 956, 352 (2016).
$(\mu^E_B / T_E > 2)$

**Dyson-Schwinger Equation (DSE):**

1): Y. X. Liu, et al., PRD90, 076006 (2014); 94, 076009 (2016).
$(\mu^E_B, T^E) = (372, 129)$ ; $(262.3, 126.3)$ MeV

2): Hong-shi Zong et al., JHEP 07, 014 (2014).
$(\mu^E_B, T_E) = (405, 127)$ MeV

3): C. S. Fischer et al., PRD90, 034022 (2014).
$(\mu^E_B, T^E) = (504, 115)$ MeV

$\mu^E_B = 262 \sim 504$ MeV, $T_E = 115 \sim 162$ MeV, $\mu^E_B / T_E = 1.74 \sim 4.38$

# STAR Detector System

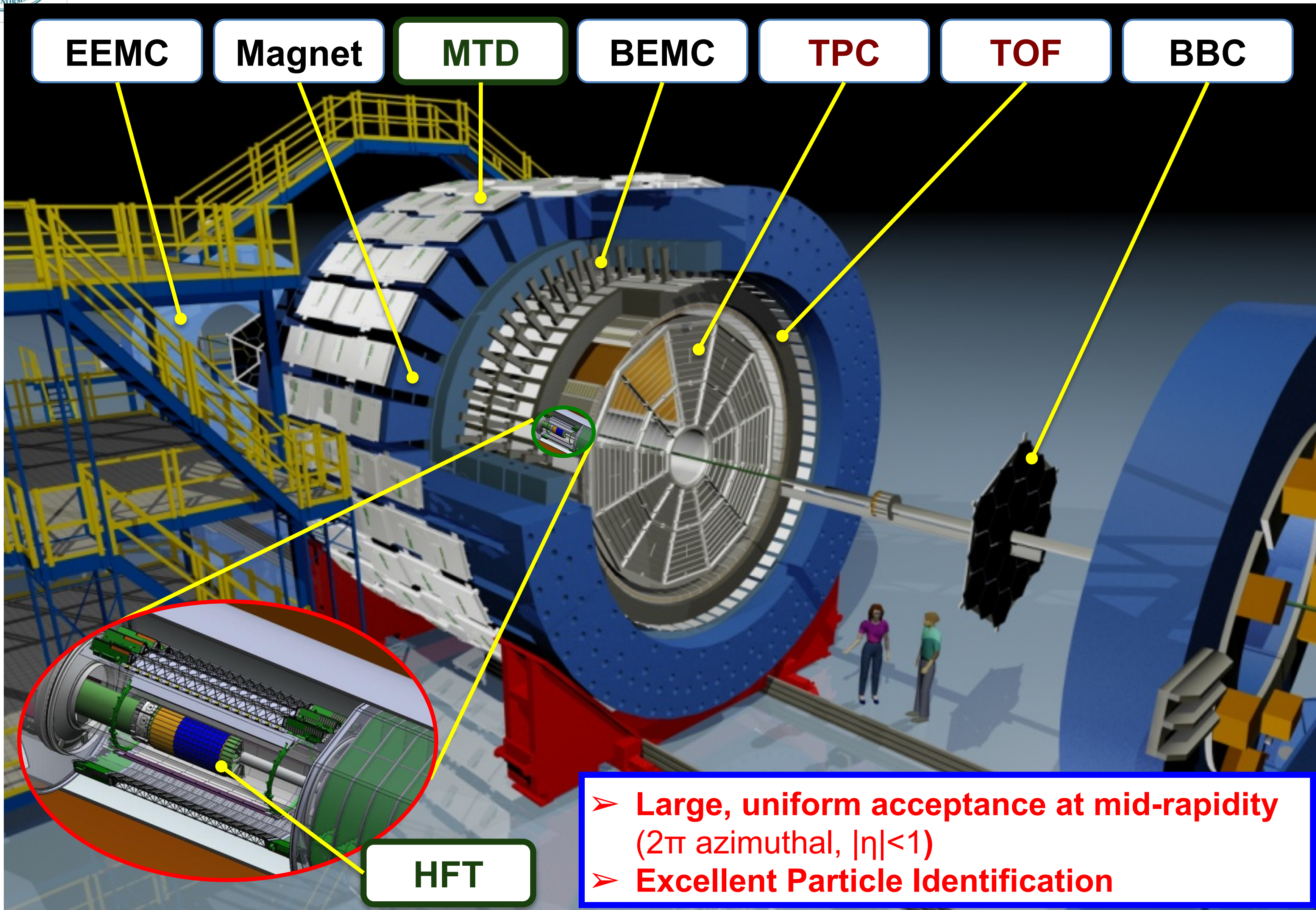


- ➢ **Large, uniform acceptance at mid-rapidity**
  (2π azimuthal, |η|<1)
- ➢ **Excellent Particle Identification**

# RHIC Beam Energy Scan-I (2010-2014)

Au+Au Collisions

| $\sqrt{s_{NN}}$ (GeV) | Events ($10^6$) | *$\mu_B$ (MeV) | *$T_{CH}$ (MeV) |
|---|---|---|---|
| 200 | 238 | 25 | 166 |
| 62.4 | 45 | 73 | 165 |
| 54.4 | 1200 | 83 | 165 |
| 39 | 86 | 112 | 164 |
| 27 | 32 | 156 | 162 |
| 19.6 | 15 | 206 | 160 |
| 14.5 | 13 | 264 | 156 |
| 11.5 | 7 | 316 | 152 |
| 7.7 | 3 | 422 | 140 |

*($\mu_B$, $T_{CH}$) : J. Cleymans et al., PRC 73, 034905 (2006)

Uniform acceptance at Mid-rapidity

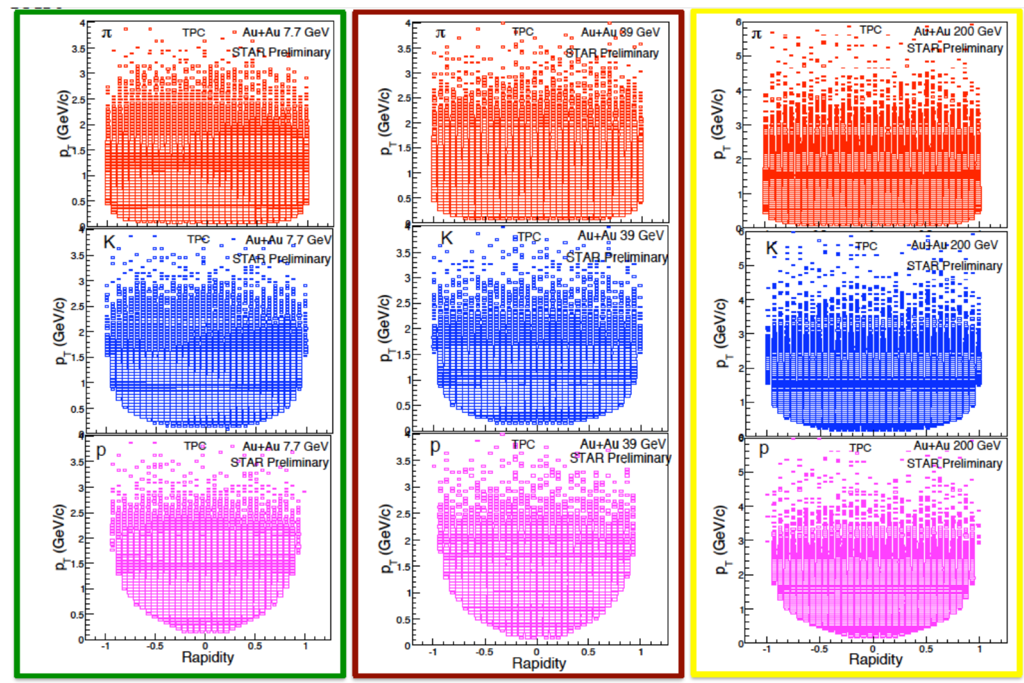


- ➢ Access the QCD phase diagram: vary collision energies/centralities. **RHIC BES-I : 20 < $\mu_B$ < 420 MeV**

# Sensitive observables !

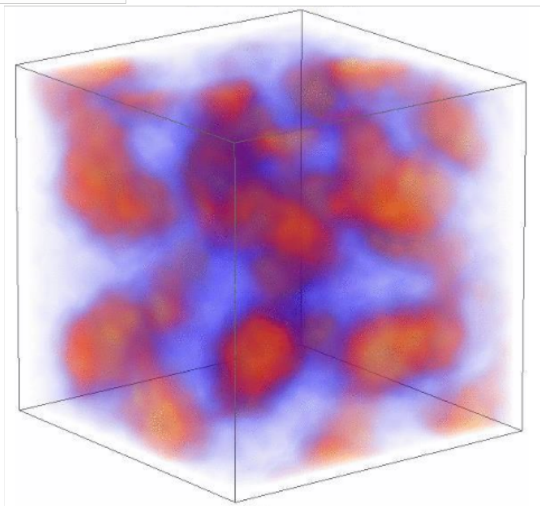

## In the vicinity of critical point

**Large density fluctuations and long range corr.**

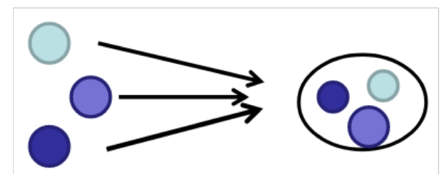

**E-by-E conserved charge (B, Q, S) fluctuations**

**Baryon clustering: light nuclei production**

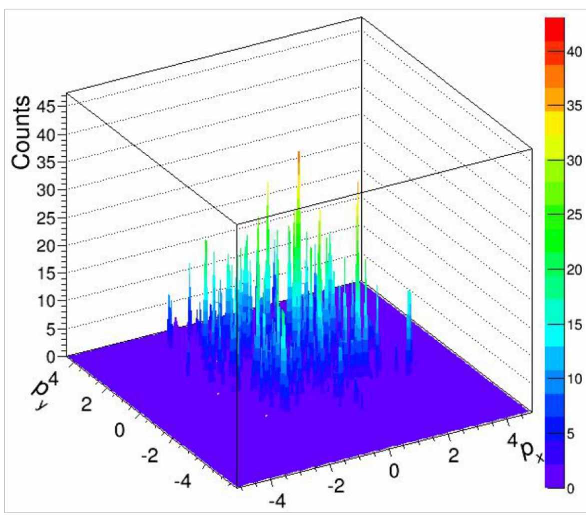


**Experimental Signatures:**

**Non-monotonic variation as a function of collision energy.**

# Higher Moments of Conserved Quantities (B, Q, S)

1. Higher order cumulants/moments: describe the shape of distributions and quantify fluctuations. (sensitive to the correlation length (ξ))

$$< \delta N >= N - < N >$$
$$C_1 = M =< N >$$
$$C_2 = \sigma^2 =< (\delta N)^2 >$$
$$C_3 = S\sigma^3 =< (\delta N)^3 >$$
$$C_4 = \kappa\sigma^4 =< (\delta N)^4 > -3 < (\delta N)^2 >^2$$

$$\left\langle (\delta N)^3 \right\rangle_c \approx \xi^{4.5}, \qquad \left\langle (\delta N)^4 \right\rangle_c \approx \xi^{7}$$

Skewness ($S$) → asymmetry

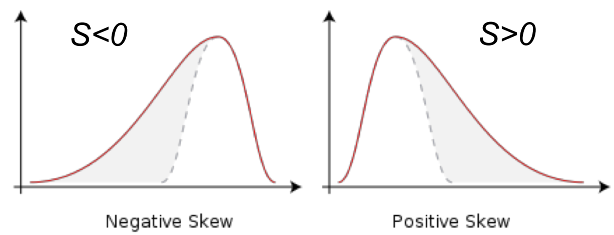


Kurtosis ($\kappa$) → Sharpness

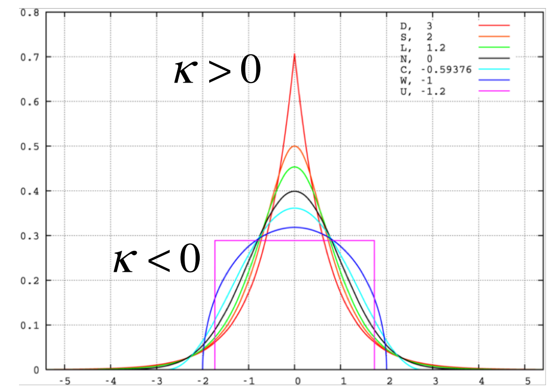


*M. A. Stephanov, Phys. Rev. Lett. 102, 032301 (2009); 107, 052301 (2011).*
*M.Asakawa, S. Ejiri and M. Kitazawa, Phys. Rev. Lett. 103, 262301 (2009).*

2. Direct connect to the susceptibility of the system.

$$\frac{\chi_q^4}{\chi_q^2} = \kappa\sigma^2 = \frac{C_{4,q}}{C_{2,q}} \qquad \frac{\chi_q^3}{\chi_q^2} = S\sigma = \frac{C_{3,q}}{C_{2,q}},$$

$$\chi_q^{(n)} = \frac{1}{VT^3} \times C_{n,q} = \frac{\partial^n (p/T \wedge 4)}{\partial(\mu_q)^n}, q = B,Q,S$$

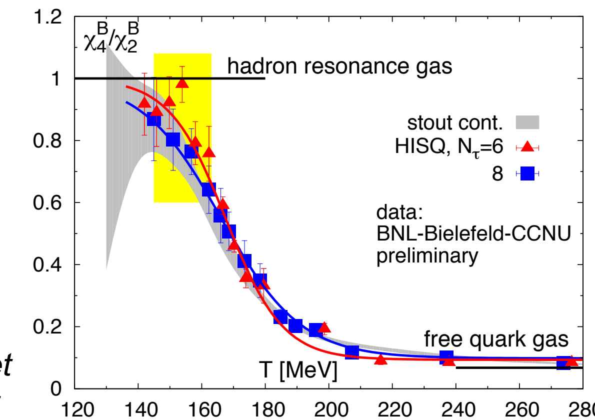


*S. Ejiri et al,Phys.Lett. B 633 (2006) 275. Cheng et al, PRD (2009) 074505. B. Friman et al., EPJC 71 (2011) 1694. F. Karsch and K. Redlich , PLB 695, 136 (2011).S. Gupta, et al., Science, 332, 1525(2012). A. Bazavov et al., PRL109, 192302(12) // S. Borsanyi et al., PRL111, 062005(13)*

# Data Analysis Methods

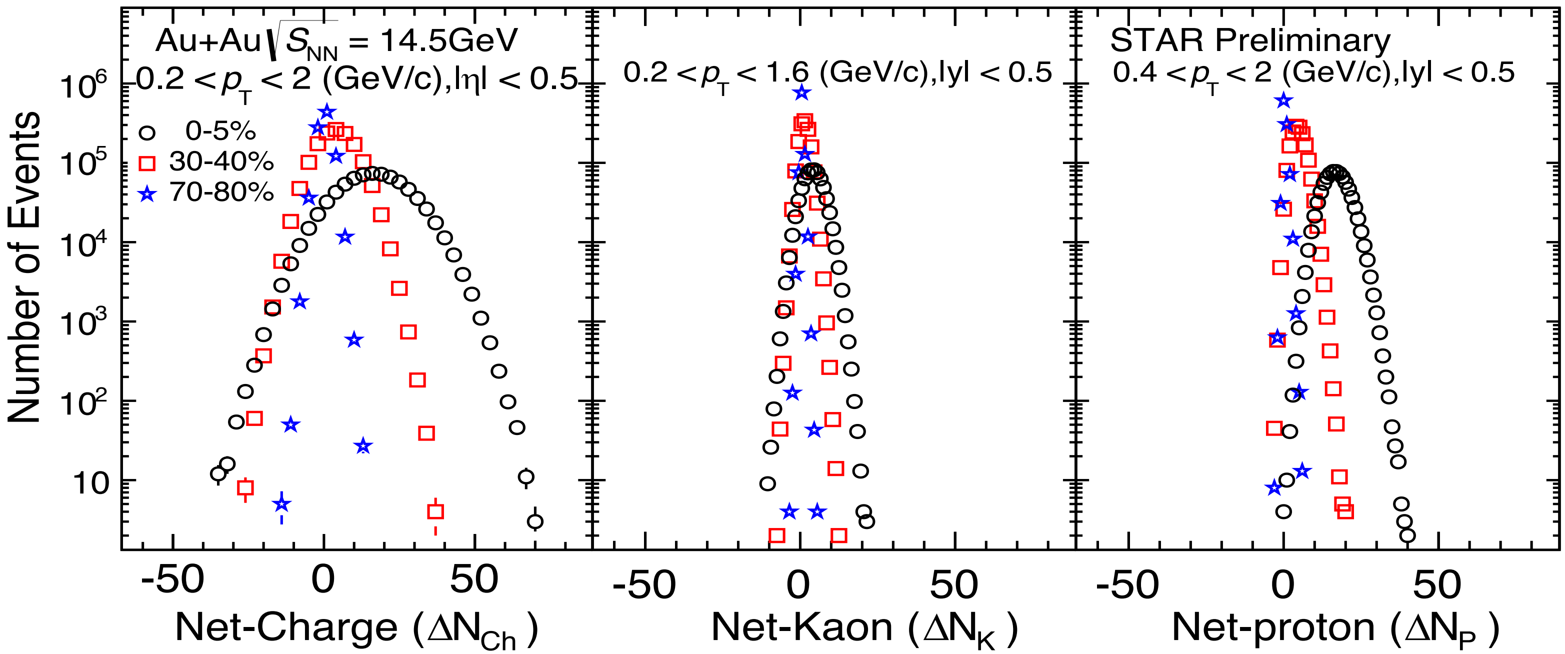


Analysis Methods used in the STAR coll.

1. Statistical errors estimation : Delta theorem or bootstrap
2. Avoid auto-correlation effects: New centrality definition.
3. Suppress volume fluctuation： Centrality bin width correction
4. Finite detector efficiency correction (binomial response func.)

*Review Article : X. Luo and N. Xu, Nucl. Sci. Tech. 28, 112 (2017).*

*X.Luo, J. Phys. G* 39, 025008 (2012); *A. Bzdak and V. Koch, PRC86, 044904 (2012); X.Luo, et al. J. Phys. G40,105104(2013); X.Luo, Phys. Rev. C 91, 034907 (2015); A . Bzdak and V. Koch, PRC91, 027901 (2015). T. Nonaka et al., PRC95, 064912 (2017). M. Kitazawa and X. Luo, PRC96, 024910 (2017). X. Luo, T. Nonaka, arXiv: 1812.10303*

# Statistical Errors Estimation and Properties

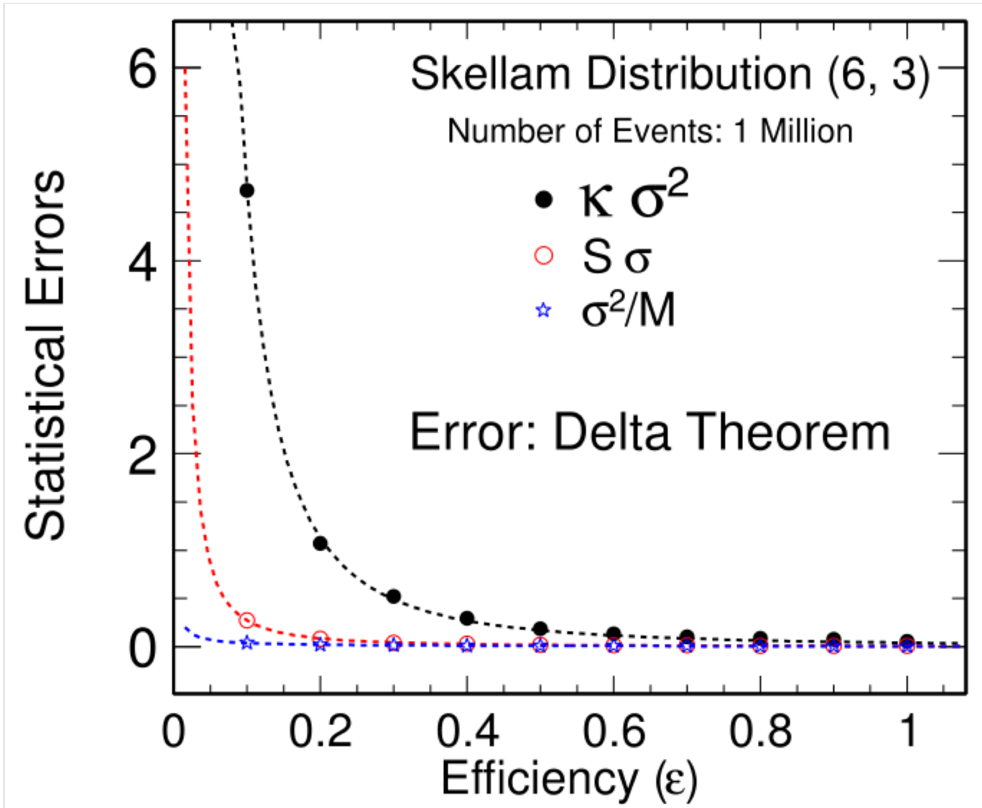


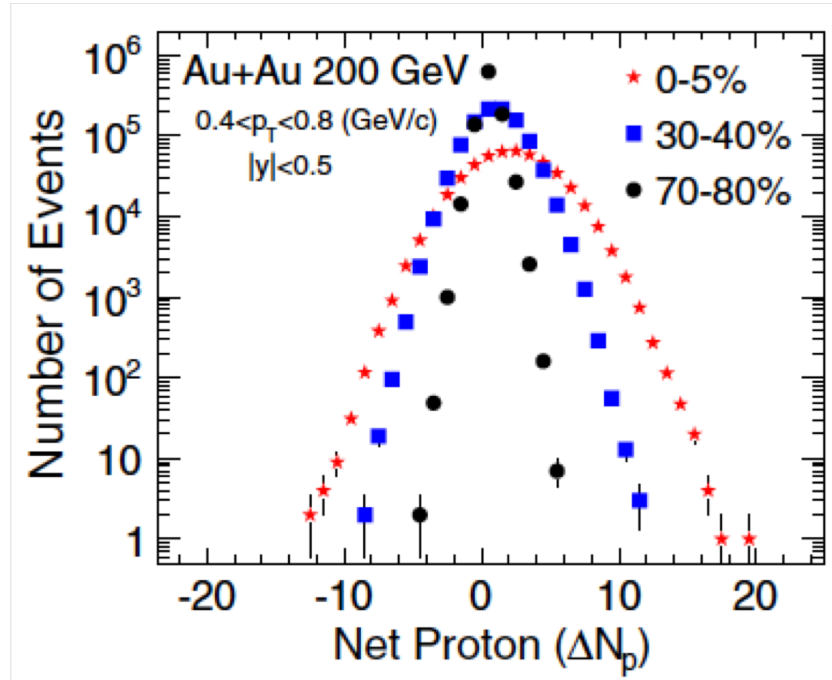


$$error(\kappa\sigma^2) \propto \frac{\sigma^2}{\varepsilon^2}\frac{1}{\sqrt{N_{evts}}}$$

*X. Luo, J. Phys. G* 39, 025008 (2012);
*X. Luo, Phys. Rev. C 91, 034907 (2015);*
*X. Luo, T. Nonaka, Phys. Rev. C 99, 044917 (2019);*

Statistical errors strongly depend on the : Width of the distributions and the detector efficiency (response function of ).

# BES-I (2010-2014) : Net-Particle Fluctuation Measurements

## Net-Proton

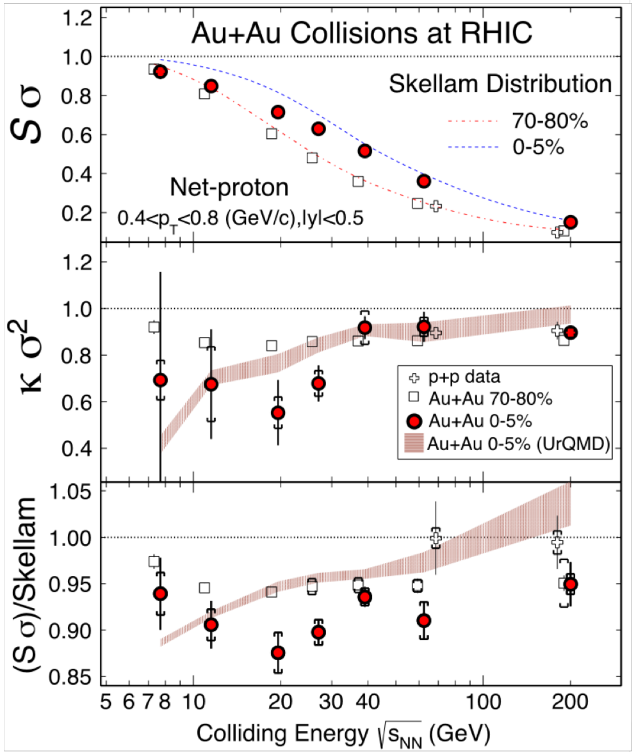


## Net-Charge

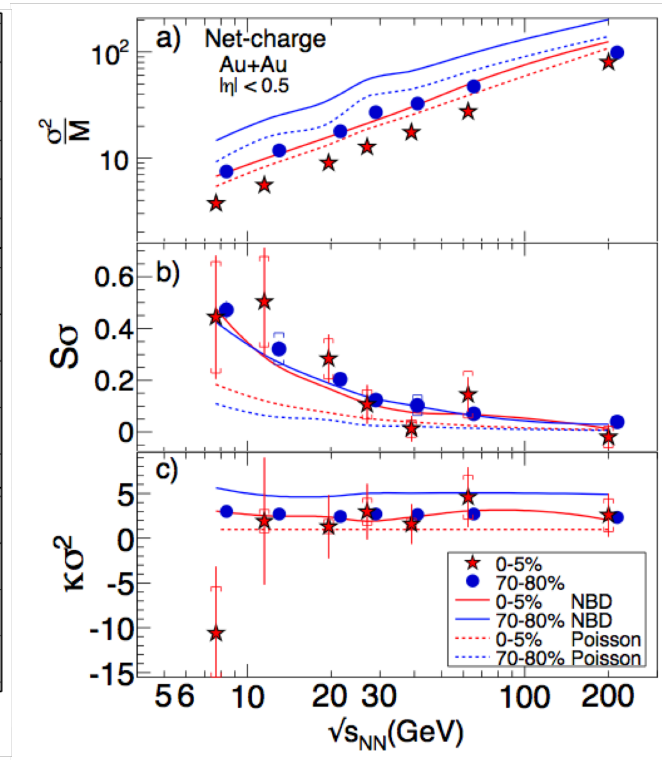


## Net-Kaon

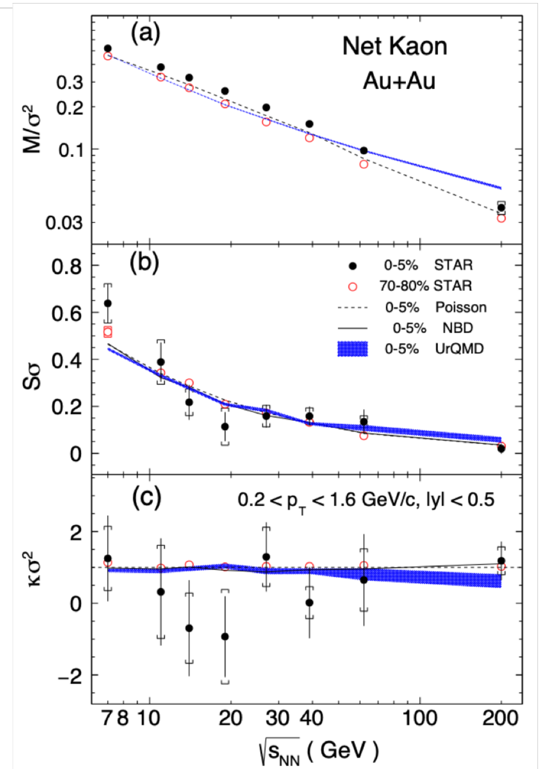


Phys. Rev. Lett. 105, 022302 (2010).
Phys. Rev. Lett. 112, 032302 (2014).

Phys. Rev. Lett. 113 092301 (2014).

Phys. Lett. B 785, 551 (2018).

# (Anti-) Proton PID and Acceptance

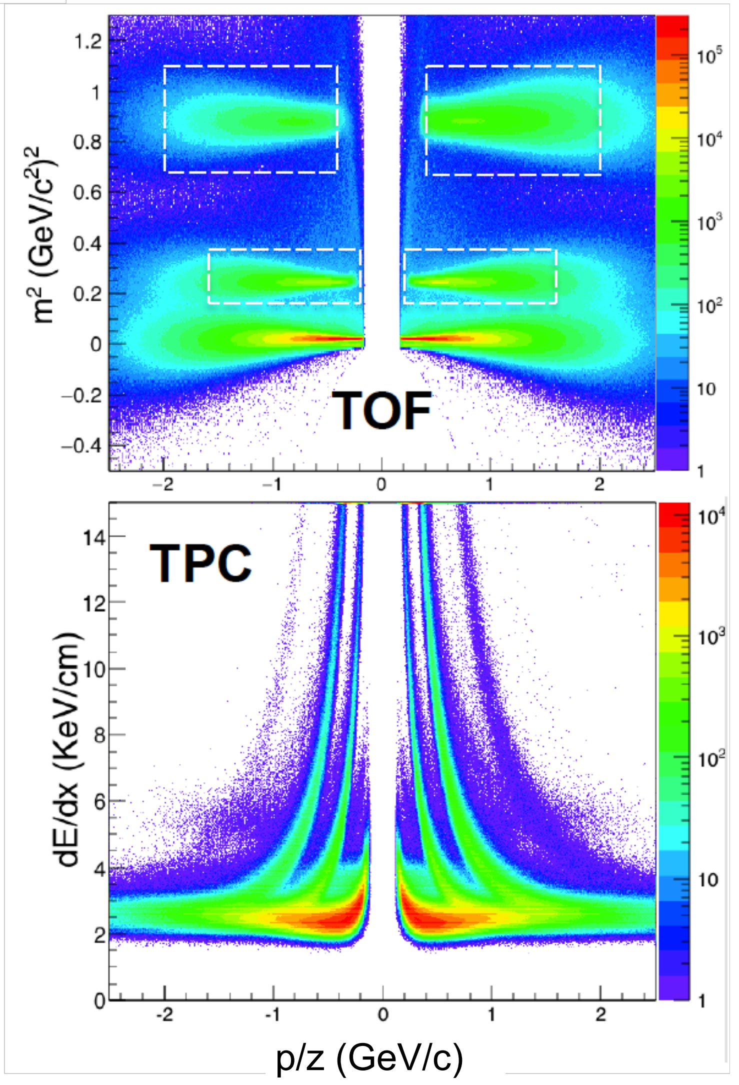


Extend the phase space coverage by TOF.

Doubled the accepted number of proton/anti-proton

*|y|<0.5, 0.4<$p_T$<0.8 (TPC PID)*

*0.8<$p_T$<2 (TPC+TOF PID)*

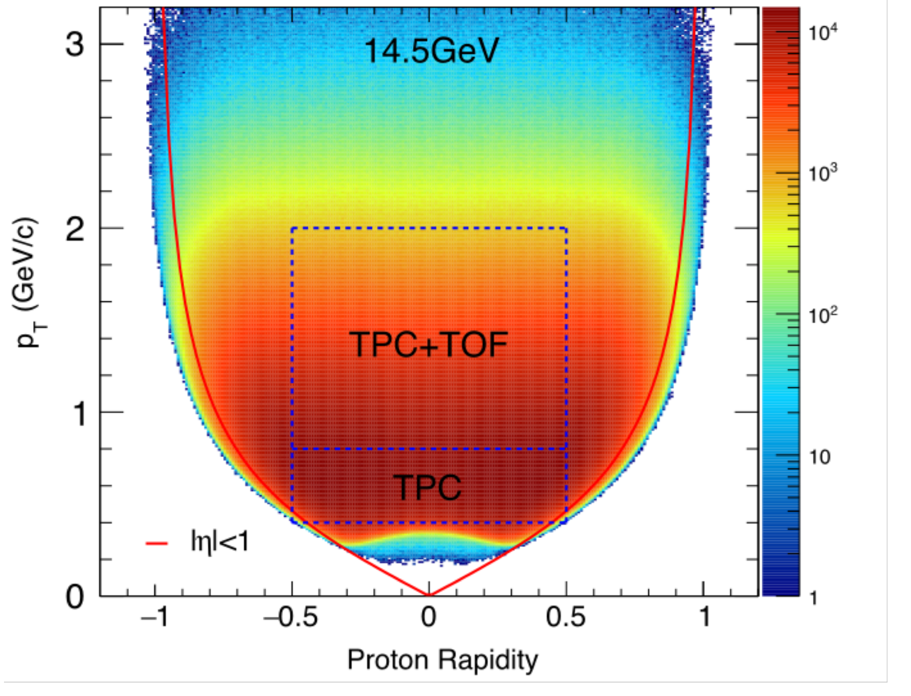


➢ Sufficiently large acceptance is important for fluctuation analysis

# (Anti-) Proton Acceptance and Efficiencies

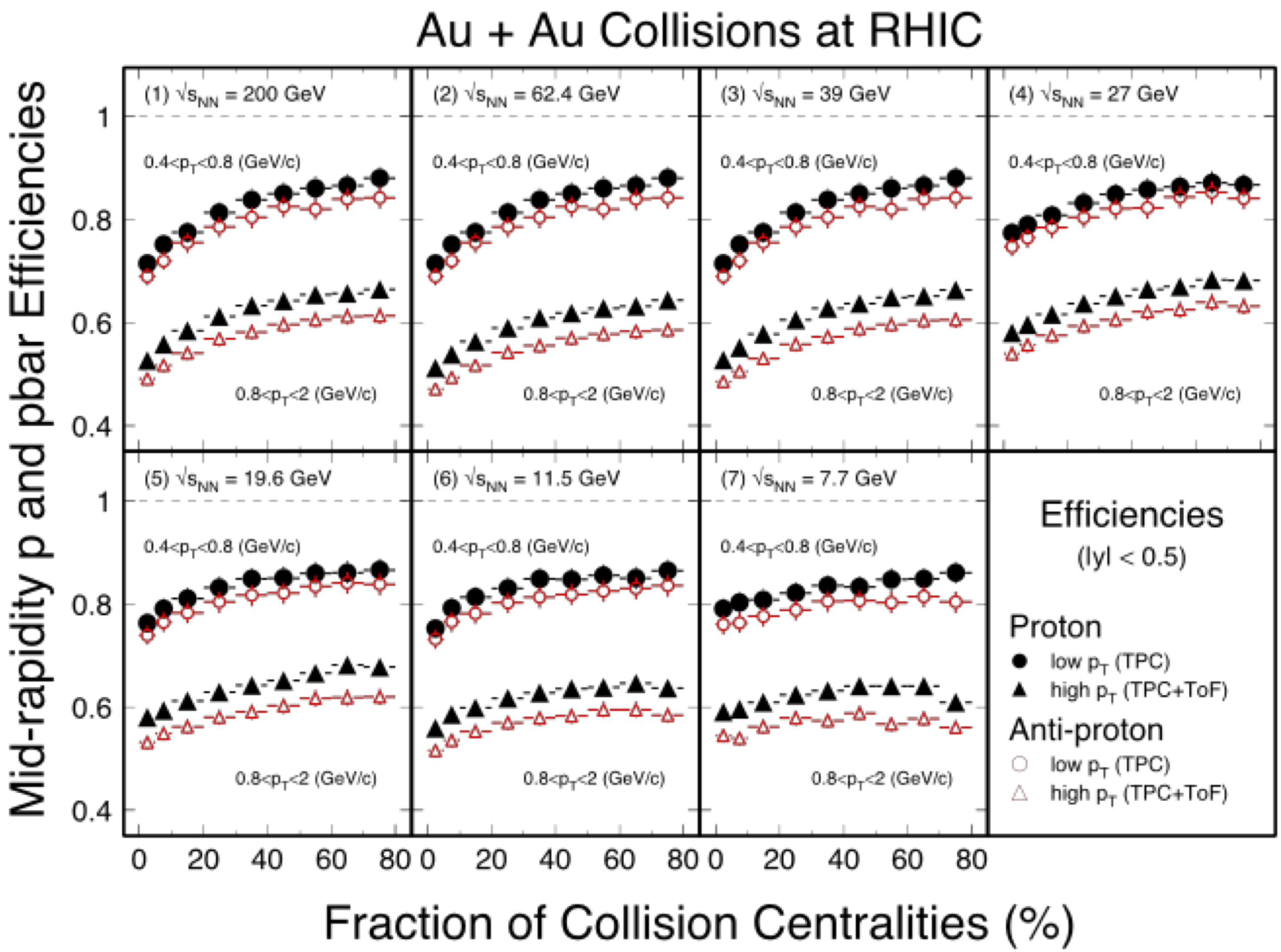


- Efficiency : Proton> Anti-proton, Low $p_T$ > High $p_T$ , low energy > High Energy, Peripheral > Central

# Results: Mean Net-p, p and pbar

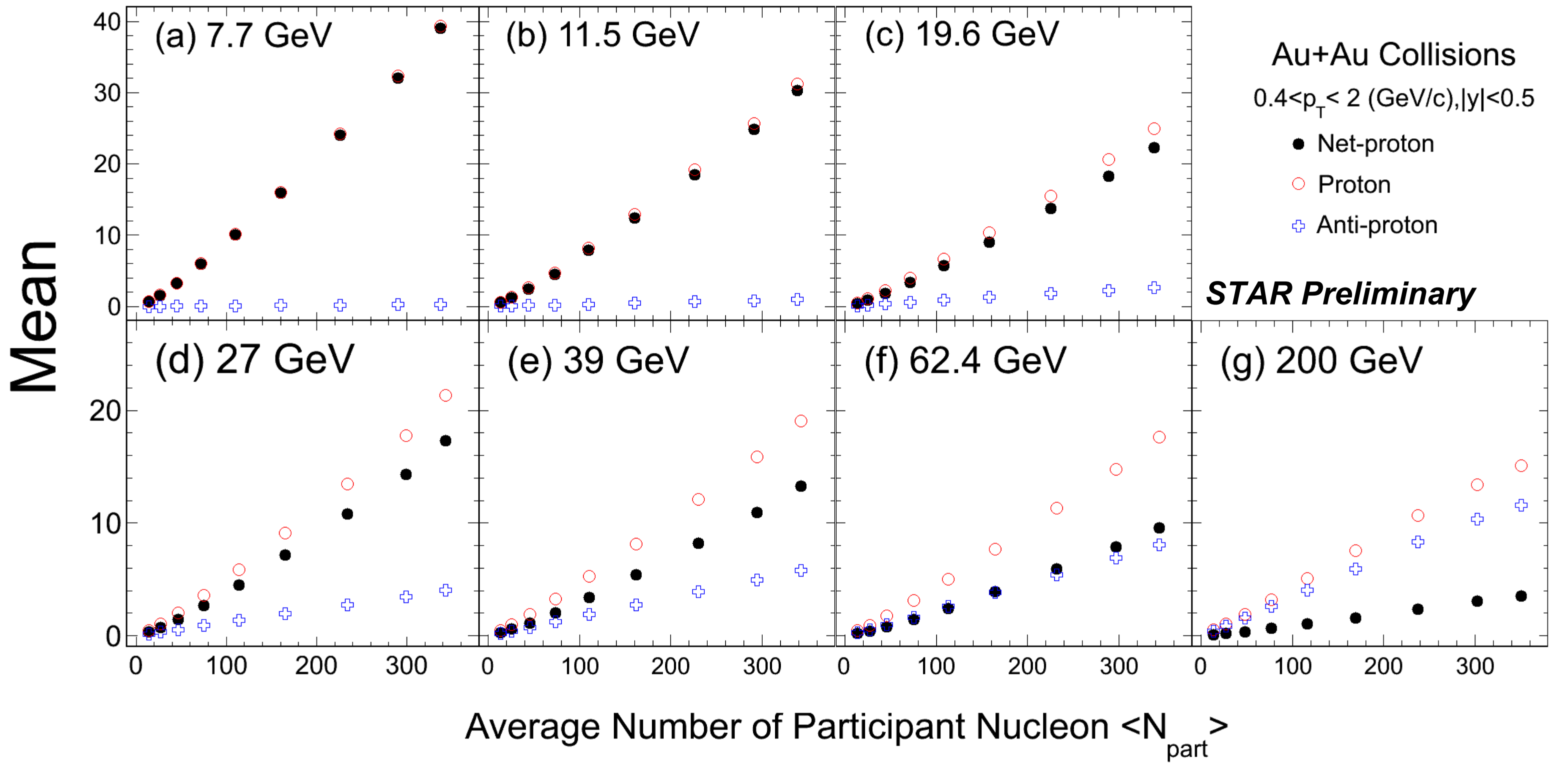


- Mean Net-proton, proton and anti-proton number increase with $\langle N_{part} \rangle$
- Net-proton number is dominated by protons at low energies and increases when energy decreases.
  (Interplay between baryon stopping and pair production)

# Higher Order Cumulants for Net-p, p, pbar

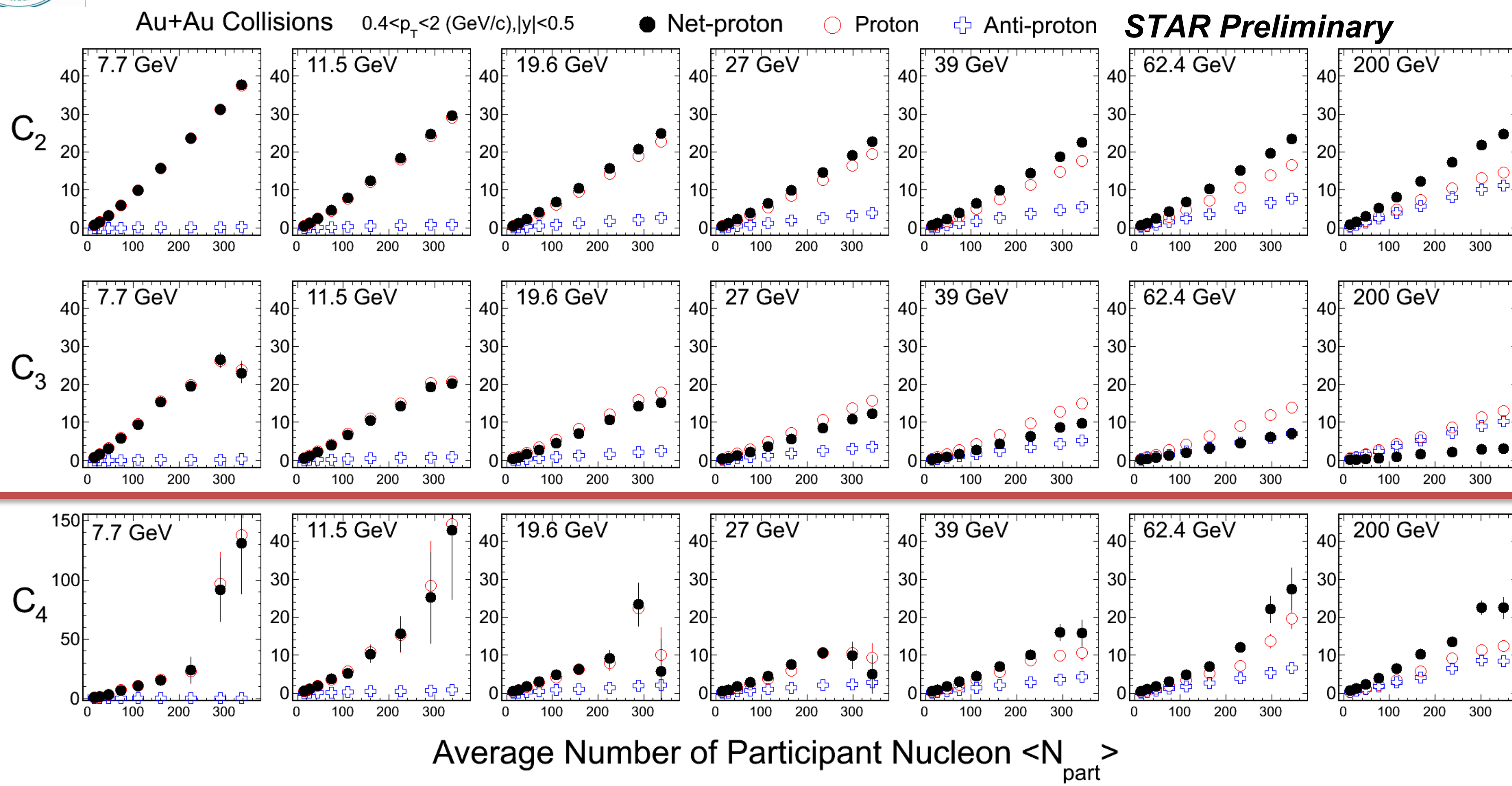


- ➢ In general, cumulants of Net-p, p and pbar are increasing with $<N_{part}>$.
- ➢ The cumulants of net-proton distributions closely follow the proton cumulants when the colliding energy is decreasing.

# Net-Proton Fluctuations

## Experimental Measure

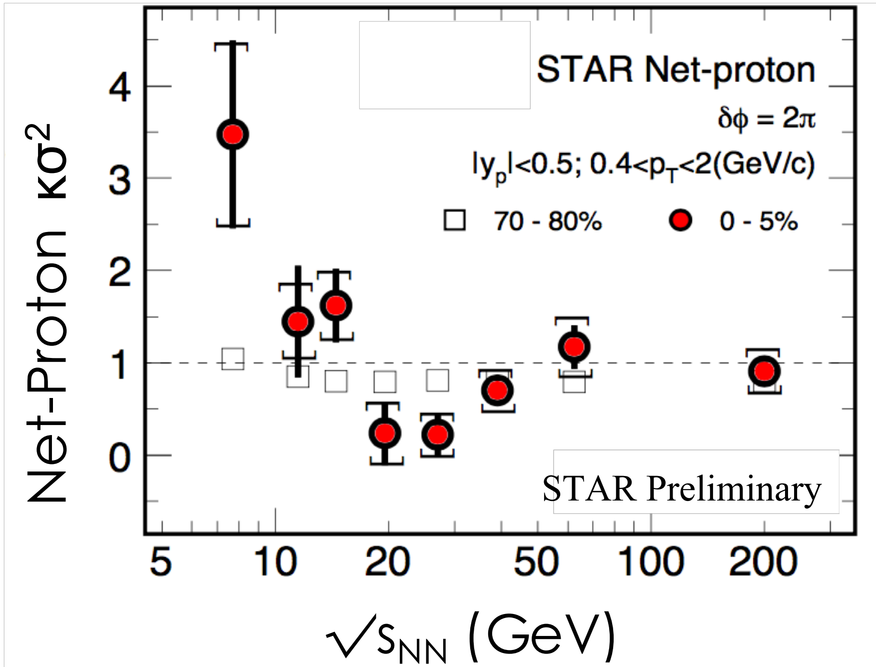


STAR: Phys. Rev. Lett. 105, 022302 (2010).
Phys. Rev. Lett. 112, 032302 (2014).
PoS CPOD2014 (2015) 019.

## Theoretical calculations

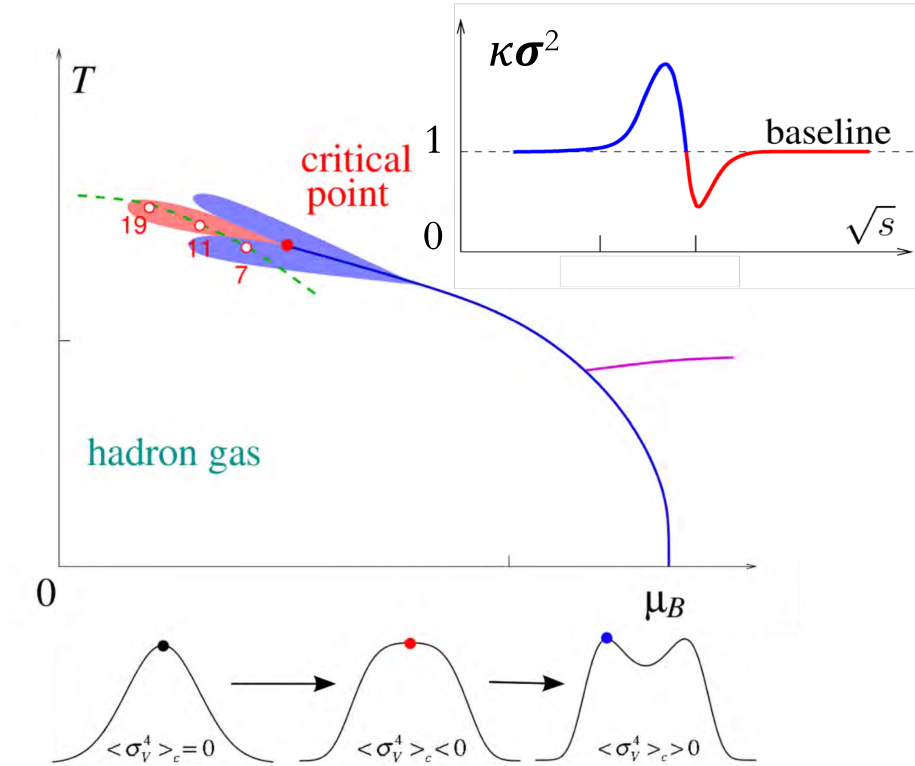


M. Stephanov, PRL107, 052301(2011)
J. Phys. G: 38, 124147 (2011).

- First observation of the non-monotonic energy dependence of fourth order net-proton fluctuations. Hint of entering Critical Region ?

# Non-critical Contributions: Transport Model Studies

## UrQMD and AMPT models

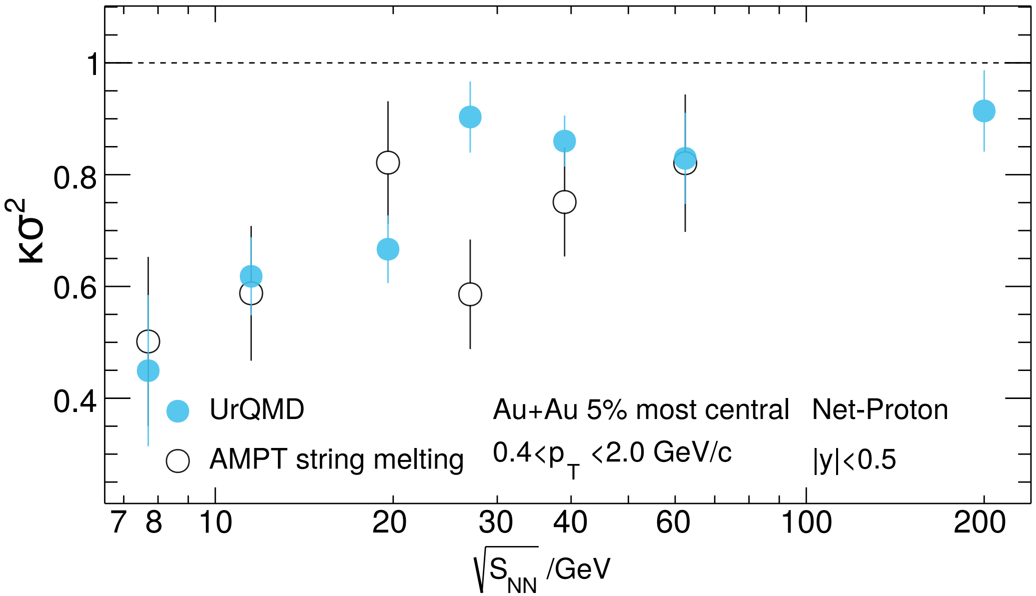


## JAM model

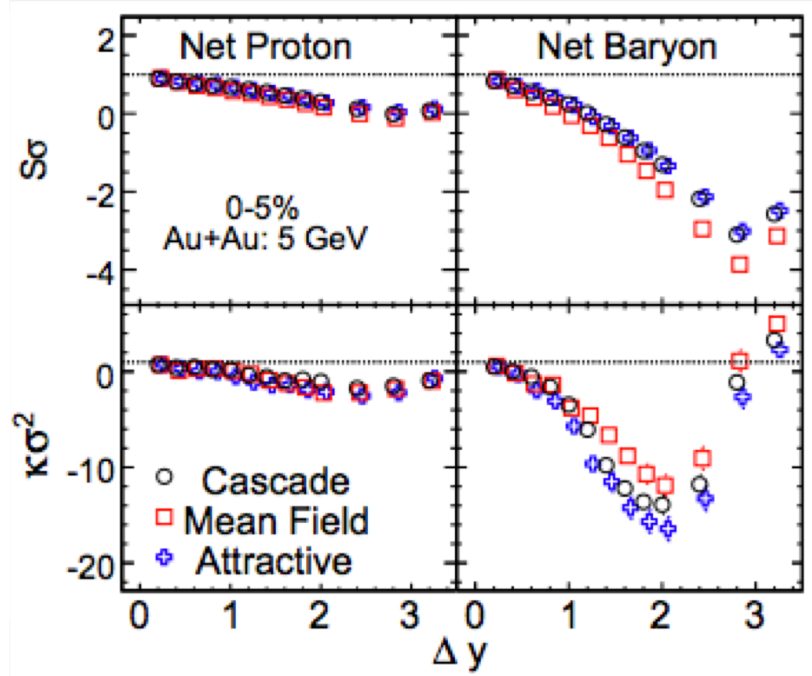


- Transport model (no CP physics) results show monotonic energy dependence: dominated by baryon number conservations
- Mean field potential can not explain the enhancement of $\kappa\sigma^2$ at low energy.

*Z. Feckova, et al., PRC92, 064908(2015). J. Xu, et. al., PRC94, 024901(2016). X. Luo et al., NPA931, 808(14), P.K. Netrakanti et al. 1405.4617, NPA947, 248(2016), P. Garg et al. PLB 726, 691(2013). S. He, et. al., PLB762, 296 (2016). S. He, X. Luo, PLB 774, 623 (2017).*

# Paper Plan

**Observation of non-monotonic variation of higher moments of net-proton distribution with collision energy in relativistic heavy-ion collisions**

**Collision of heavy-ions at relativistic energies have established the formation of two distinct phases of matter in the temperature (T) versus baryonic chemical potential ($\mu_B$) phase diagram of strong interactions. The two phases corresponds to the high $T$ de-confined state of quarks and gluons (basic building blocks of visible matter) and their confined state of hadrons at a lower $T$, both at small $\mu_B$ . A dedicated program to study the properties (viscosity, opacity, conductivity, vorticity, etc.) of the phases and to look for details related to the phase structures (nature of phase transition and critical point) associated with this Quantum Chromodynamics (QCD) phase diagram, by varying the collision energy, was launched in the year 2010 at the Relativistic Heavy-Ion Collider (RHIC) facility. Here we present results related to the search for critical point (CP) in the QCD phase diagram. When the system with N particles passes through the critical region it gets endowed with special properties, like the density fluctuations increase dramatically as a positive power of N and when away from the region the density fluctuations are small $\sim N^{-1/2}$. These fluctuations which are related to the correlation length and the susceptibilities of the system are captured by the moments of the multiplicity distributions. As the strongly interacting system produced in heavy-ion collisions are of short length and time scales, non-monotonic variations in the collision energy dependence of higher order moments of conserved number (Baryon, Charge or Strangeness) distributions is the experimental signature for the existence of the CP in the QCD phase di-**

Short Paper :

Target Journal: Nature Physics

1. The paper draft is almost ready.
2. Analysis note ready.
3. Paper Proposal : done

Next step:
Request PWGC Preview and GPC

Long Paper :

Figures for long paper are ready.
Will make paper proposal within 1 month.

# The 2nd-order Off-diagonal Cumulants

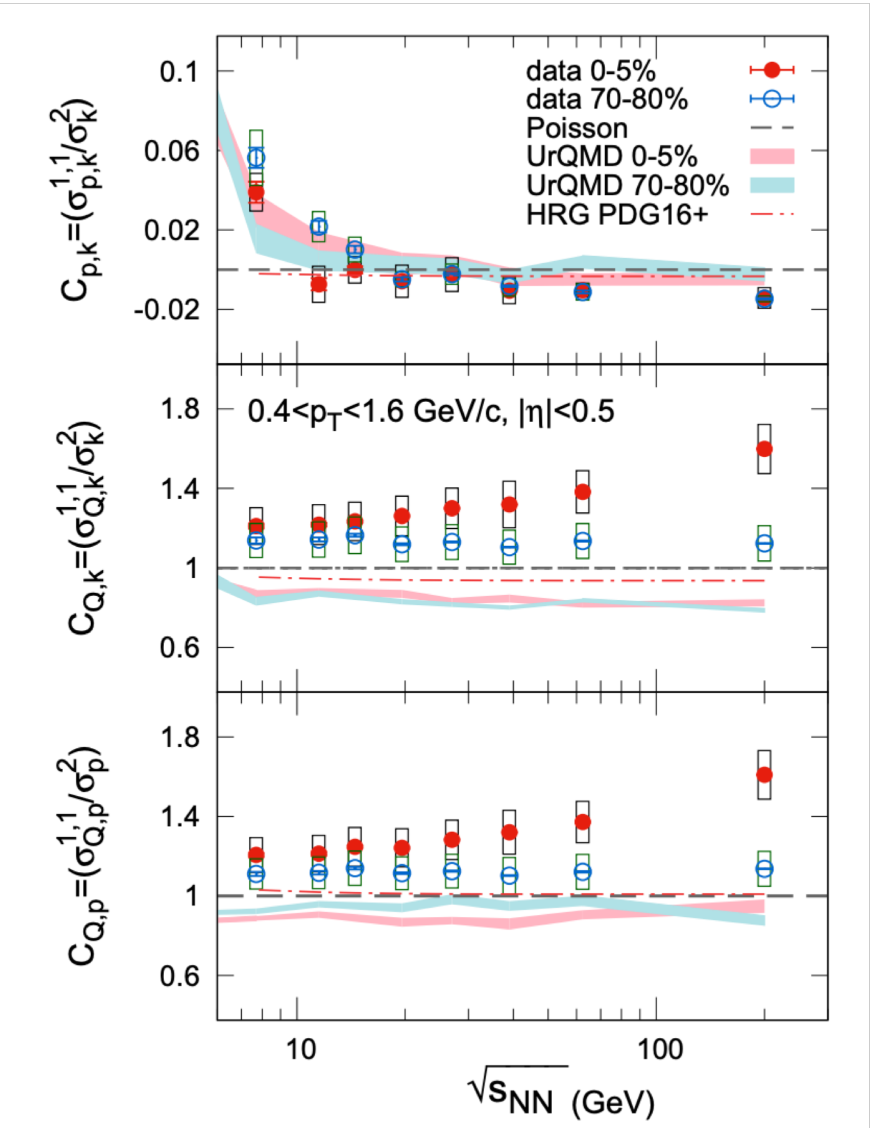


STAR, arXiv: 1903.05370

$$\sigma^2_{x,y} = \langle xy \rangle - \langle x \rangle \langle y \rangle$$

$$C_{x,y} = \frac{\sigma^{1,1}_{x,y}}{\sigma^2_y}$$

- Normalized p-k correlation is positive at low energies and negative at high energies, which are also consistent with UrQMD.

- Significant excess is observed in Q-k and Q-p with respect to the Poisson baseline and UrQMD.

# New Observable for CP: Light Nuclei Production

**Near CP or 1st order phase transition, baryon density fluctuation become large.**

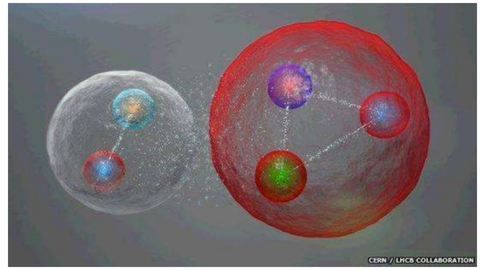


**Light nuclei production**

**(Baryon Clustering)**

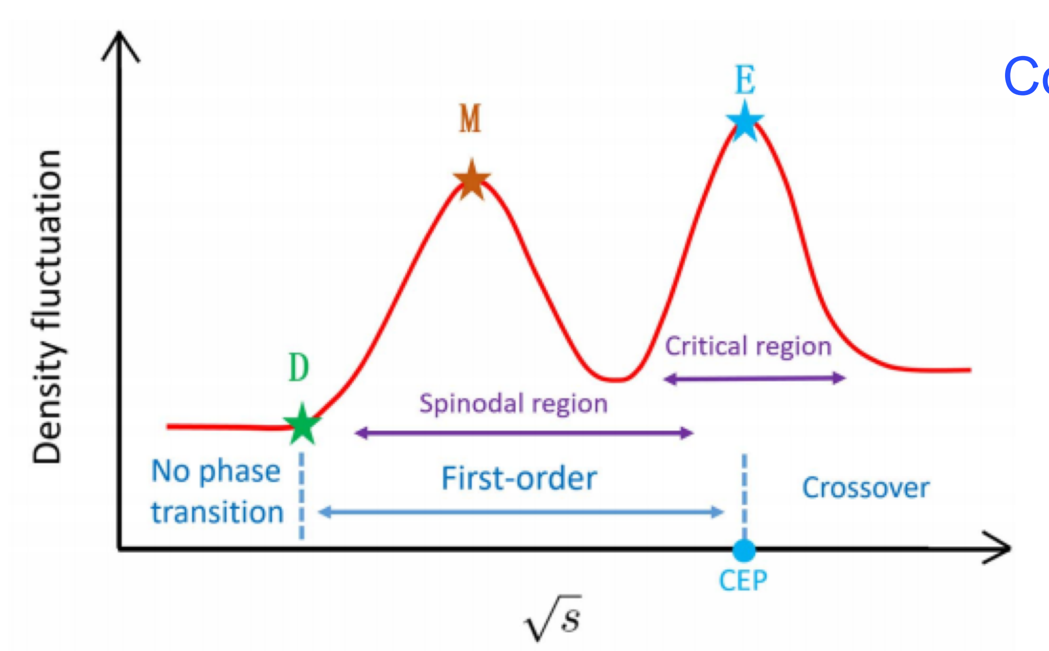


Coalescence + nucleon density flu.

$$N_d = \frac{3}{2^{1/2}}\left(\frac{2\pi}{m_0 T_{\rm eff}}\right)^{3/2} N_p \langle n\rangle (1+\alpha\Delta n),$$

$$N_{^3H} = \frac{3^{3/2}}{4}\left(\frac{2\pi}{m_0 T_{\rm eff}}\right)^{3} N_p \langle n\rangle^2 [1+(1+2\alpha)\Delta n],$$

$$N_t \cdot N_p / N_d^2 \approx g(1+\Delta n)$$

Neutron density fluctuations:

$$\Delta n = \langle(\delta n)^2\rangle / \langle n\rangle^2$$

K. J. Sun, L. W. Chen, C. M. Ko, Z. Xu, Phys. Lett. B774, 103 (2017).
K. J. Sun, L. W. Chen, C. M. Ko, J. Pu, Z. Xu, Phys. Lett. B781, 499 (2018).
Edward Shuryak and Juan M. Torres-Rincon, arXiv:1805.04444

# Deuteron and triton production from BES-I at RHIC

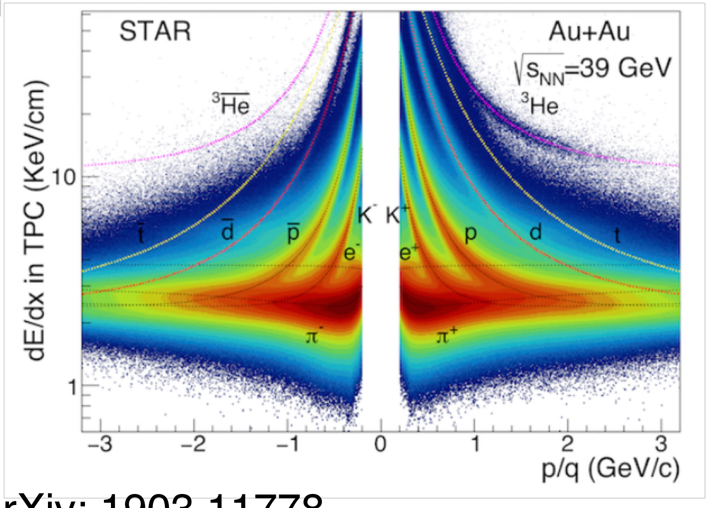


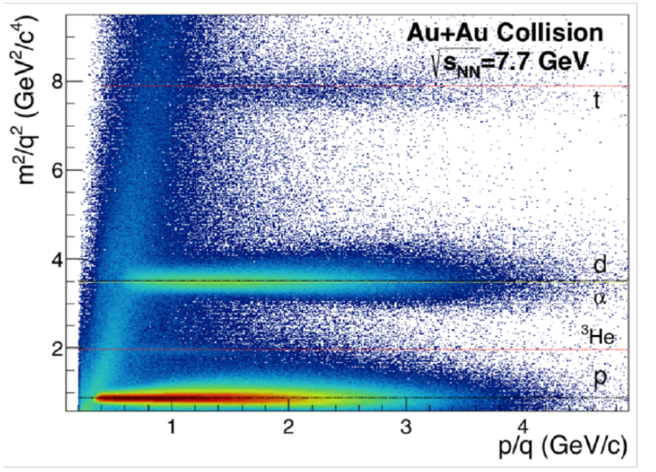


STAR, arXiv: 1903.11778

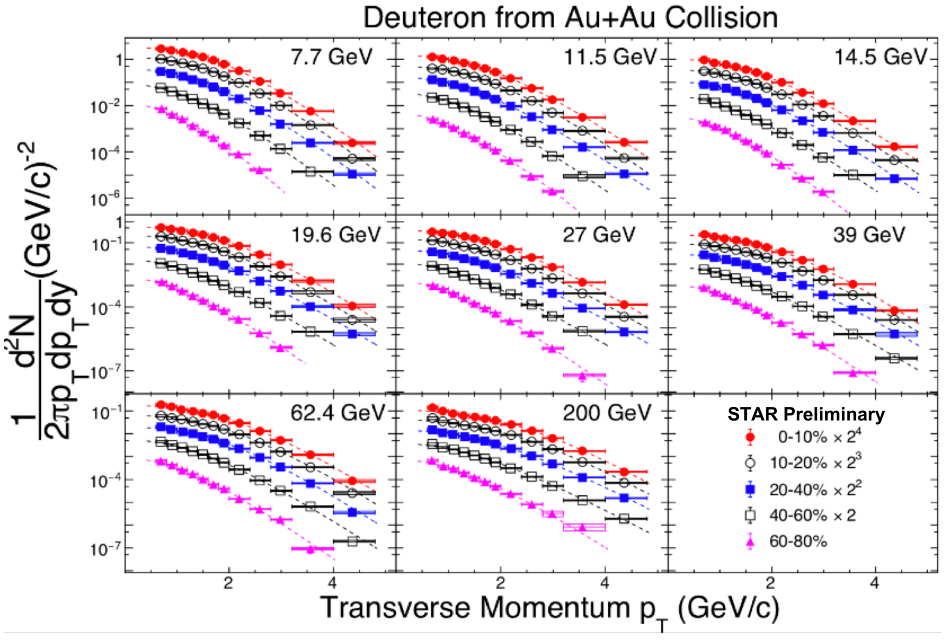


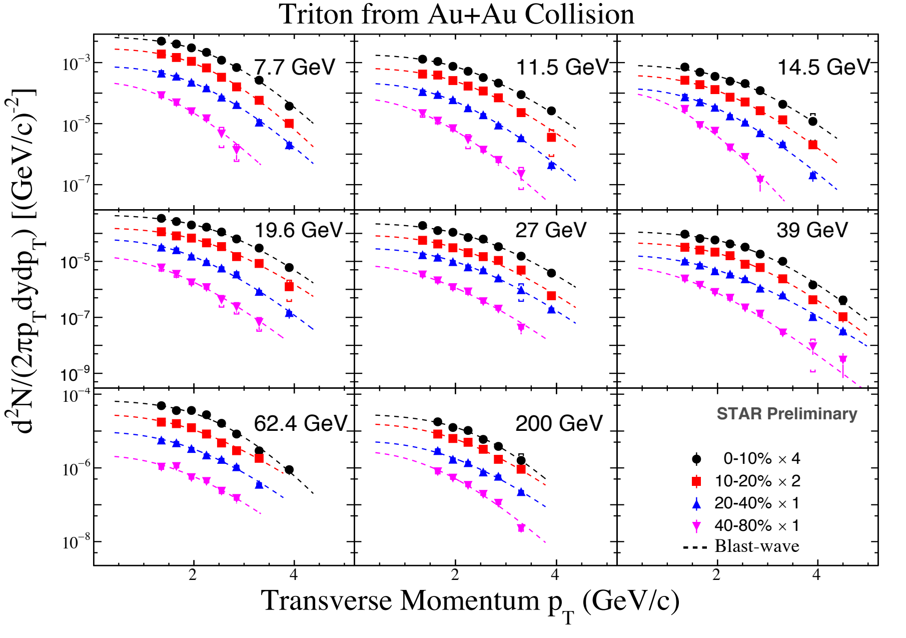

# Light Nuclei Yield Ratio Vs. Thermal model

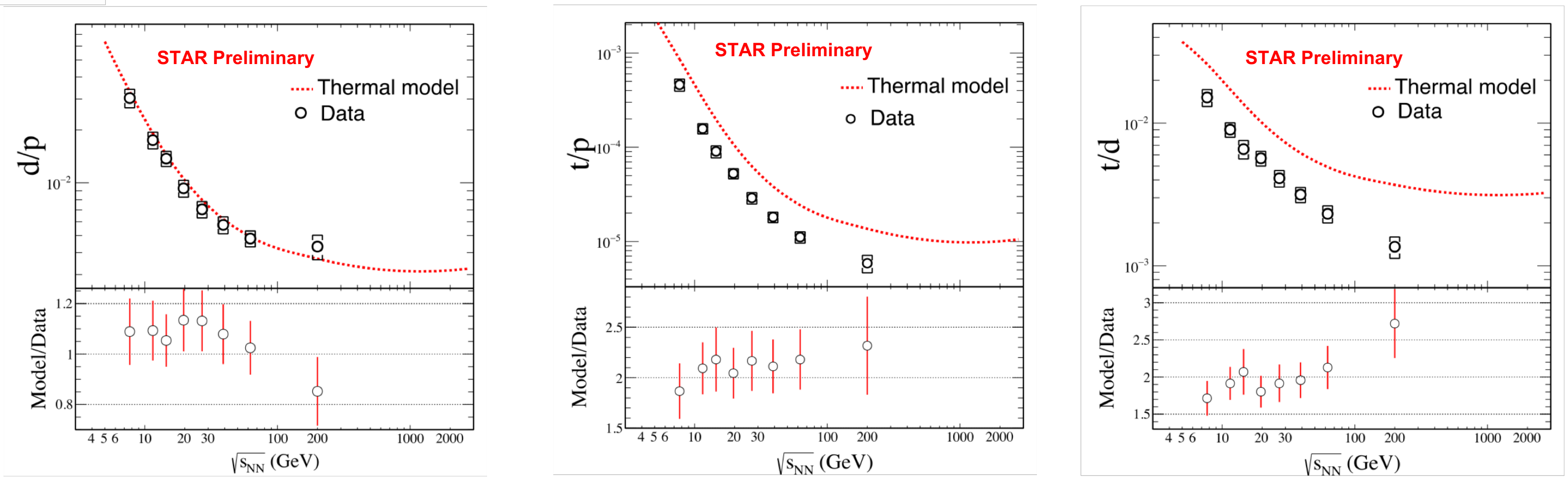


➢ At RHIC energies, thermal model can describe the d/p ratios, but can not describe the t/p, t/d ratios.

➢ If deuteron is formed at very late stage via nucleon cola., why it can be described by thermal model ?

# Nucleon Density Fluctuations

- The particle ratios of light nuclei is sensitive to the **nucleon density fluctuation** at kinetic freeze-out. This conclusion is based on **coalescence model.**

$$N_d = \frac{3}{2^{\frac{1}{2}}}\left(\frac{2\pi}{m_0 T_{eff}}\right)^{3/2} N_p\langle n\rangle(1+\alpha\Delta n) \quad N_t = \frac{3^{3/2}}{4}\left(\frac{2\pi}{m_0 T_{eff}}\right)^{3} N_p\langle n\rangle^2[1+(1+2\alpha)\Delta n]$$

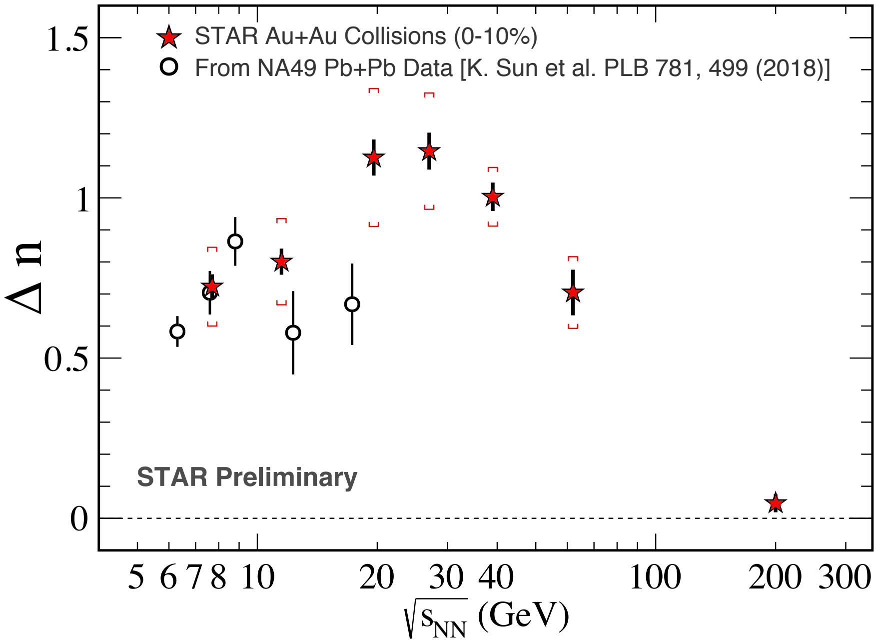


Dingwei Zhang， NN2018

If assume $\alpha$=0.

$$\frac{\langle(\delta n)^2\rangle}{\langle n\rangle^2} = \Delta n = \frac{1}{g}\frac{N_t N_p}{N_d^2} - 1$$

$N_t$ : Triton yield, $N_d$ : Deuteron yield
$N_p$ : Proton yield

Neutron density fluctuation $\Delta n$ shows a non-monotonic behavior on collision energy. Peak around 20 GeV.


K. J. Sun，L. W. Chen, C. M. Ko, Z. Xu, Phys. Lett. B774, 103 (2017).
K. J. Sun，L. W. Chen, C. M. Ko, J. Pu, Z. Xu, Phys. Lett. B781, 499 (2018).
Edward Shuryak and Juan M. Torres-Rincon, NPA 982, 831 (2019)

# STAR Upgrades for BES Phase-II (2019-2021)

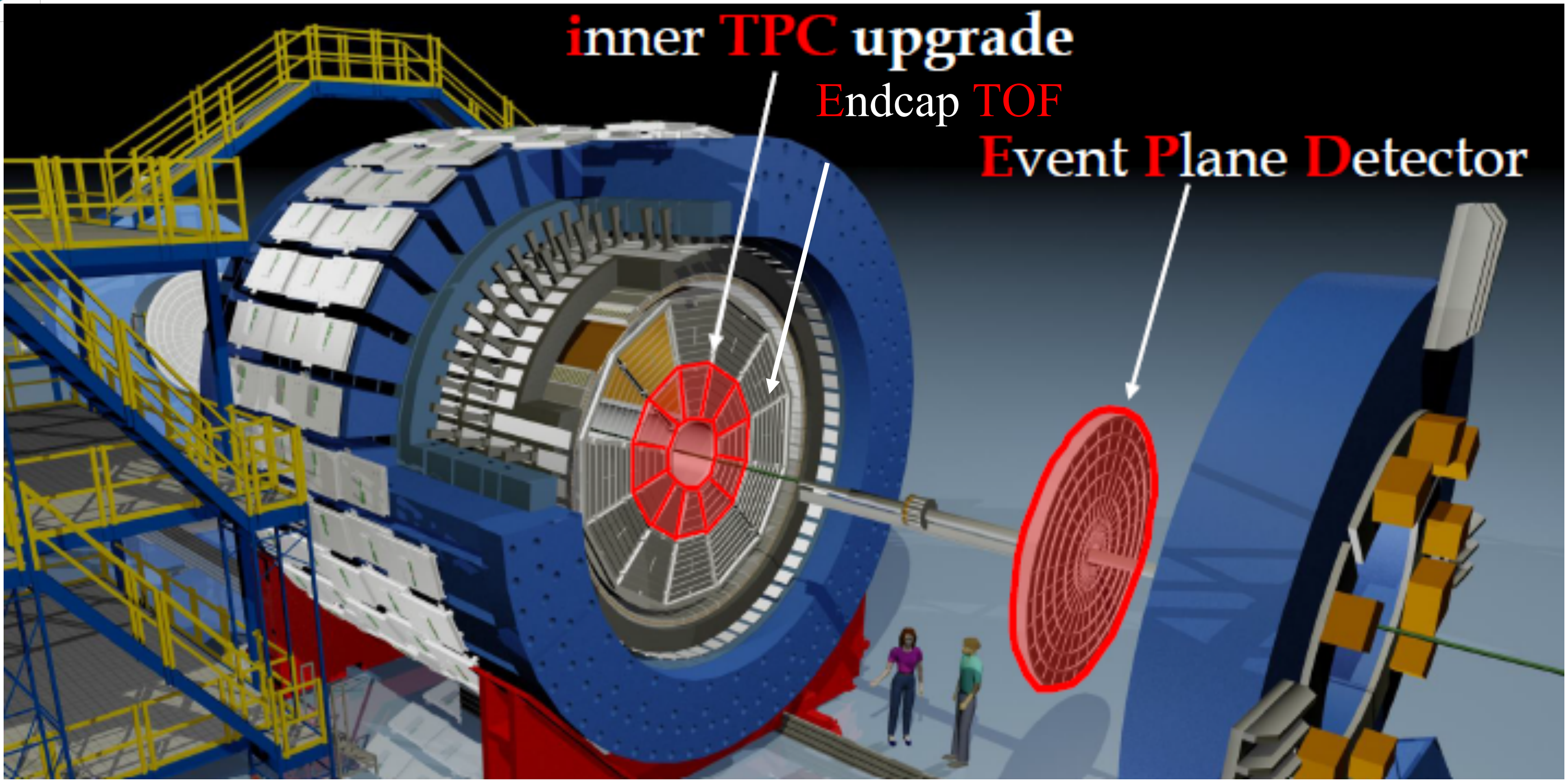


- ➢ **Enlarge Acceptance** : $\eta$ coverage from 1.0 to 1.5
- ➢ **Improve dE/dx and forward PID**
- ➢ **Improve centrality/event plane determination**

**iTPC, EPD, eTOF Upgrade complete**
**Dedicated runs at : 2019-2021**

# BES-II at RHIC (2019-2021)

| √$s_{NN}$ (GeV) | Events ($10^6$) | BES II / BES I |
|---|---|---|
| 200 | 238 | 2010 |
| 62.4 | 45 | 2010 |
| 54.4 | 1200 | 2017 |
| 39 | 86 | 2010 |
| 27 | 32 | 2011 |
| 19.6 | **400** / 15 | **2019** / 2011 |
| 14.5 | **300** / 13 | **2019** / 2014 |
| 11.5 | **230** / 7 | **2020** / 2010 |
| 9.2 | **160** / 0.3 | **2020** / 2008 |
| 7.7 | **100** / 3 | **2020-202** / 2010 |

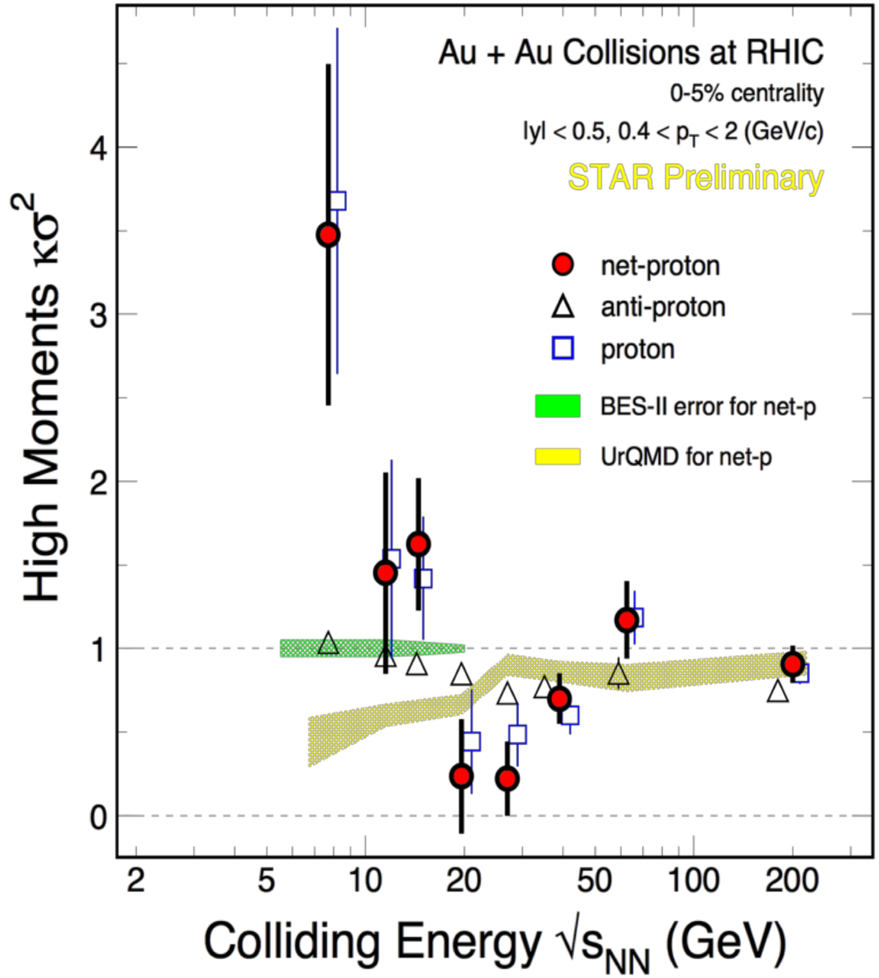


**BES-II 19.6 GeV data taking is finished and now is taking 14.5 GeVdata.**

# 3D Event Display in TPC at STAR

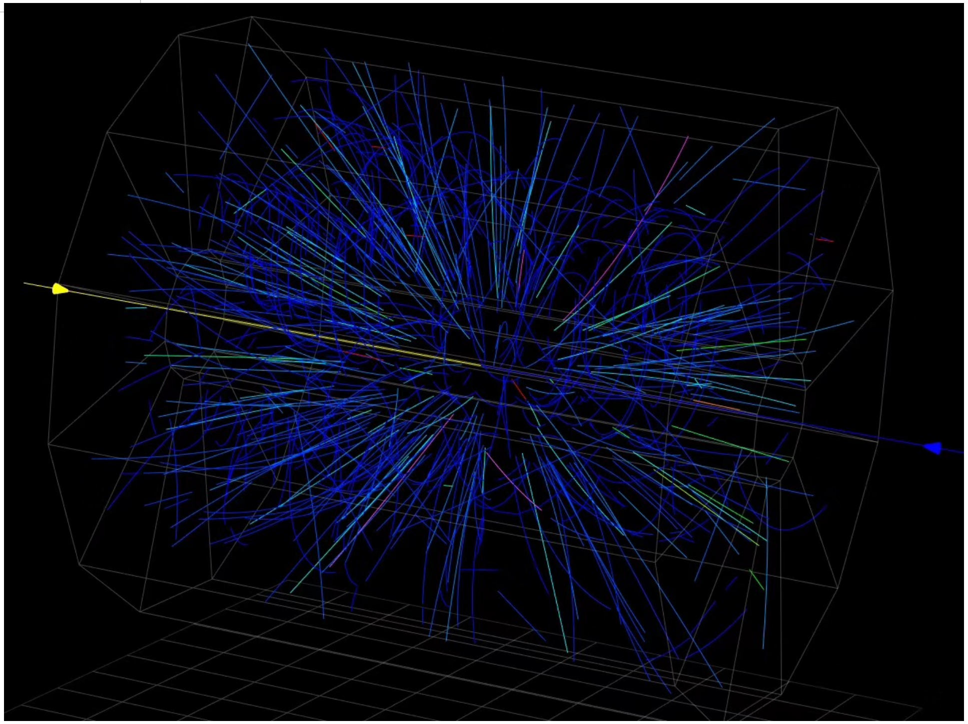

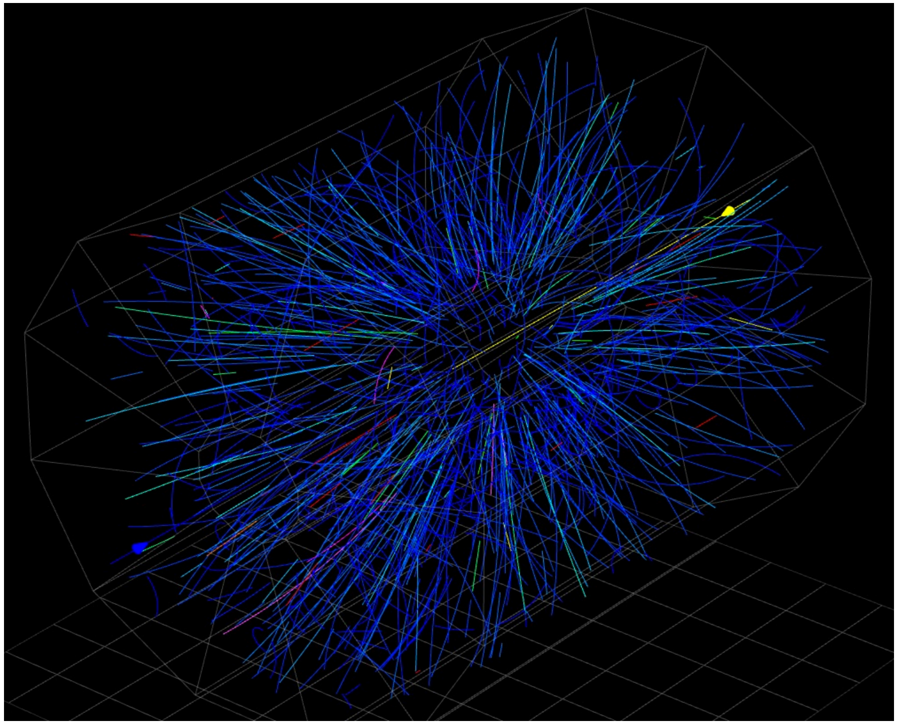

**Au+Au collisions at 19.6 GeV.** **Au+Au collisions at 14.5 GeV.**

BES-II data taking is ongoing !

# FXT Experiments at STAR (2018-2020)

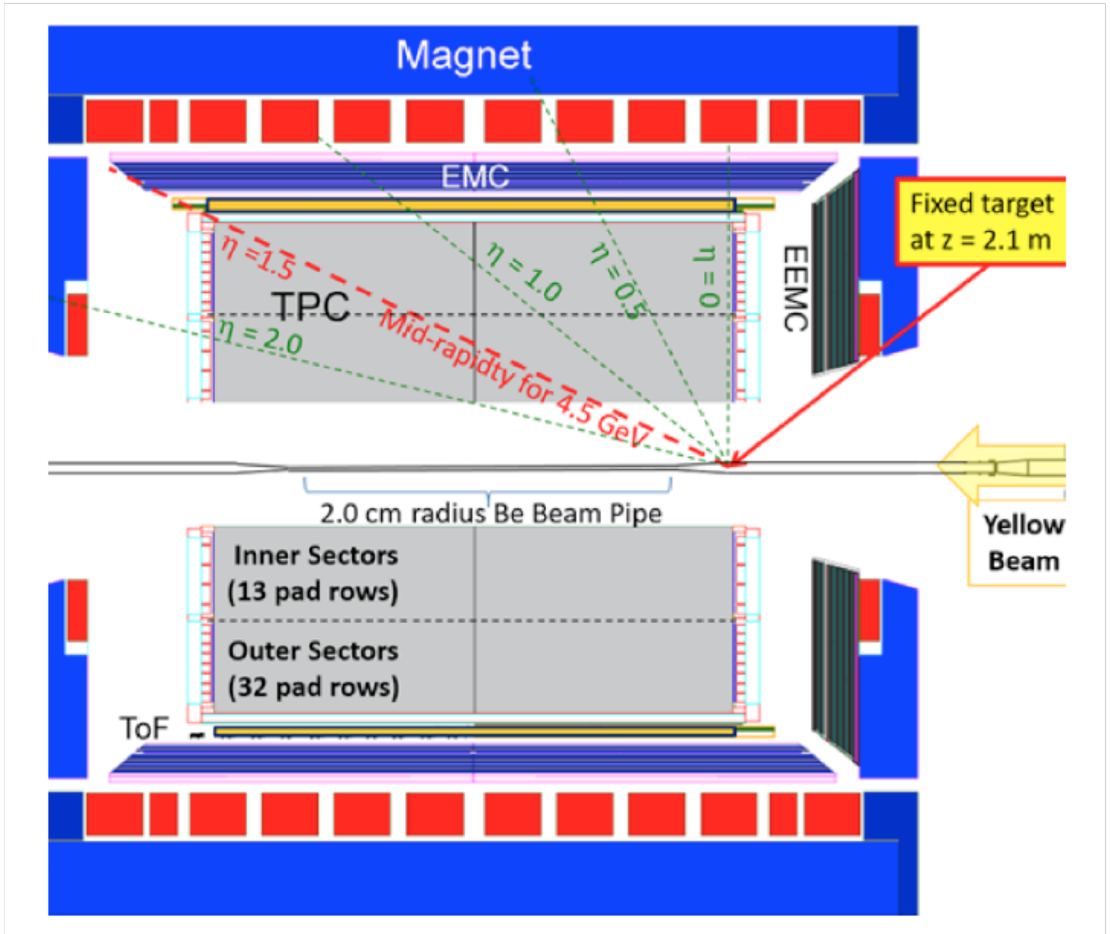


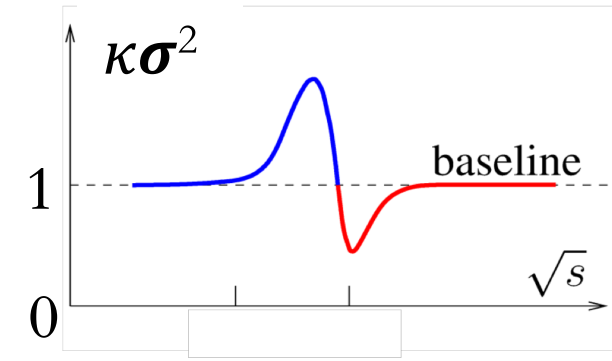


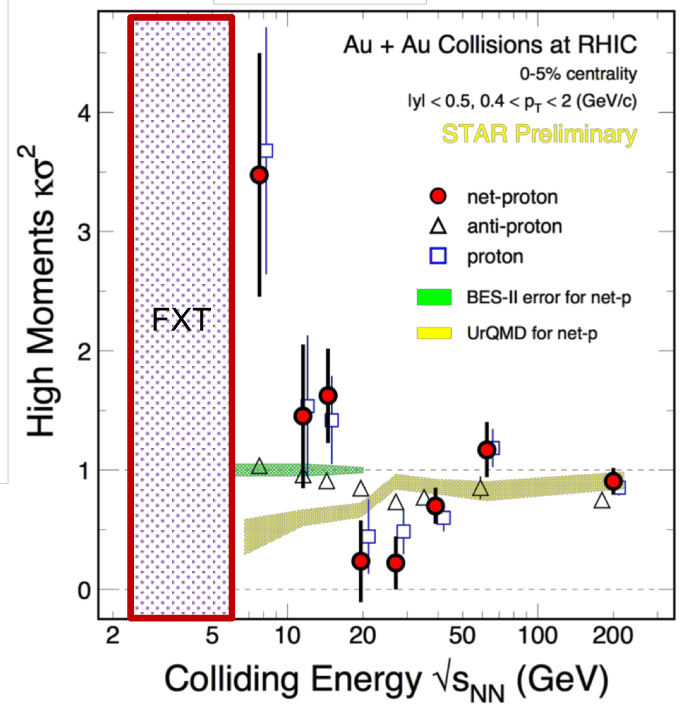


FXT Data Taking Plan：

2018: Au+Au :3 GeV (>100 million events)

2019-2020: Au+Au: 7.3, 6.2, 5, 4.5, 4, 3.5 GeV

# Summary

**Explore the QCD phase structure with Beam Energy Scan**

- Fourth order net-proton fluctuations ($C_4/C_2$) in central Au+Au collisions shows non-monotonic energy dependence, with a minimum around 20-30 GeV. Hint of entering the critical region.

- Neutron density fluctuations in 0-10% central Au+Au collisions shows non-monotonic energy dependence with a peak around 20-30 GeV.
 Hint of entering the critical region.

- In BES-II, we can study the QCD phase structure with high precision at $\sqrt{s_{NN}}$ = 7.7-19.6 GeV (collider mode) and 3-7.3 GeV (Fix-target mode)

**Stay tuned for RHIC BES-II !!**

*Thank you !*

# ALICE Data Vs. Thermal Model

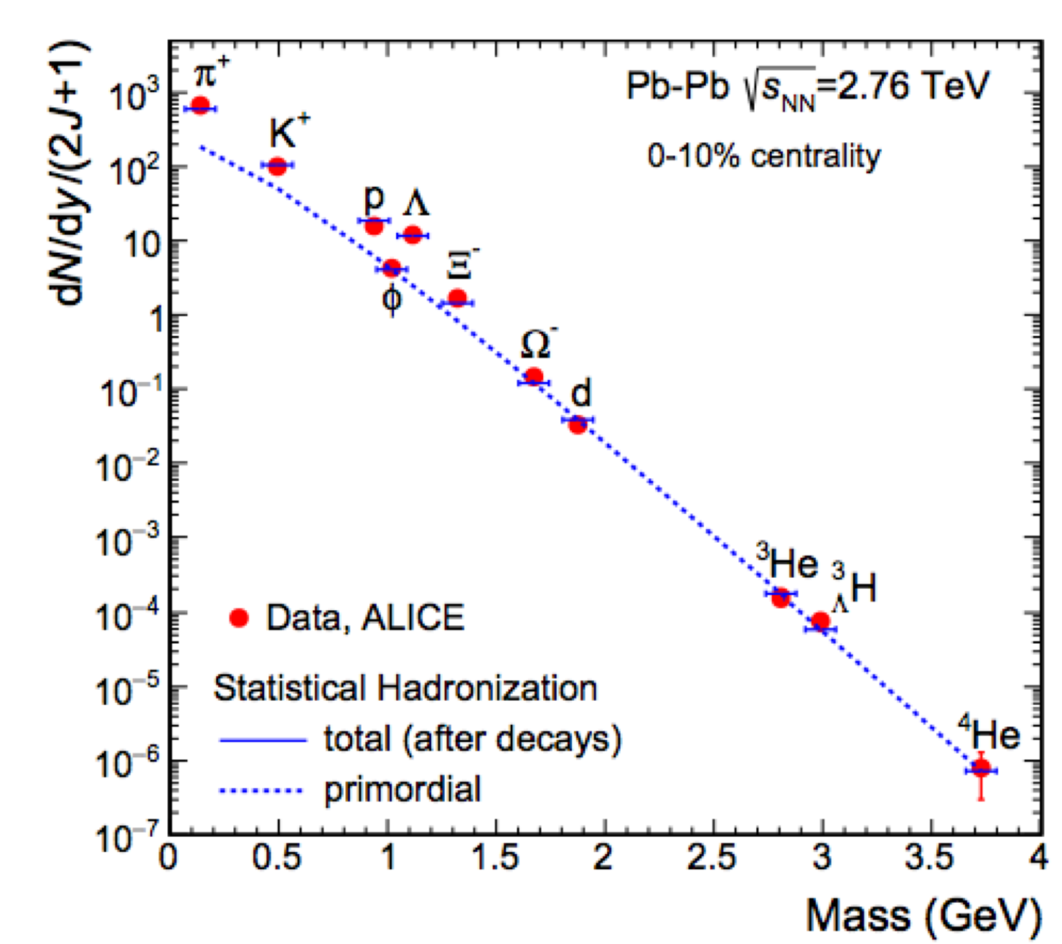


Why the yield of triton and even alpha can be well described by thermal model at LHC energies But not at RHIC energies ?

**Different production mechanism of light nuclei at RHIC and LHC energies ??**

A. Andronic, P. Braun-Munzinger, K. Redlich, J. Stachel, Nature 561, 321 (2018).